

1
2
3
4 Manuscript 30 September 2021/PSt submitted to AGU Space Weather journal.
5
6
7

8 **The polar cap (PC) index: PCS version based on Dome-C data**

9
10 Peter Stauning
11 Danish Meteorological Institute, Copenhagen, Denmark
12 Mail: pst@dmi.dk
13
14

15 **Abstract**

16 The standard Polar Cap (PC) indices, PCN (North) based on magnetic data from Qaanaaq in
17 Greenland and PCS (South) based on data from Vostok in Antarctica, have been submitted from the
18 Arctic and Antarctic Research Institute (AARI) in St. Petersburg, Russia, the Danish
19 Meteorological Institute (DMI), and the Danish Space Research Institute (DTU Space) in different
20 versions. In order to consolidate PCS indices based on Vostok data or replace poor or missing index
21 data, derivation procedures have been developed to generate alternative PCS index values based on
22 data from Dome Concordia (Dome-C) magnetic observations from epoch 2009-2020 of solar cycle
23 24. The reference levels and calibration parameters needed for calculations of Dome-C-based PCS
24 values in post-event and real-time versions are defined and explained in the present work.
25 Assessments of the new PCS index have shown its unprecedented high relevance. Part of the
26 methods used here such as the quiet reference level construction and the correlation and regression
27 procedures used for calculations of scaling parameters deviate from corresponding features
28 considered inadequate of the IAGA-endorsed PC index derivation methods.
29
30

31 **Description in plain text.**

32 The polar cap (PC) indices are derived from magnetic variations measured in the central northern
33 and southern polar caps. They represent the coupling between the solar wind and the magnetosphere
34 providing power to space weather disturbances such as strong electric currents in the polar
35 ionosphere. These currents may in turn generate upper atmosphere heating which may disturb
36 satellite orbits and induce electric currents and voltages in conducting structures at ground level.
37 During the strong events the geomagnetically induced currents (GIC) may cause power line failures
38 in important subauroral power grids. The geomagnetic disturbance level is conveniently monitored
39 through the PC indices. However, due to the harsh Arctic and Antarctic environments,
40 measurements or transmissions of magnetic data may be impeded. Thus, alternative PC index
41 sources are needed to ensure reliable space weather monitoring. The present work defines and
42 describes an alternative PCS (South) index based on measurements from the Antarctic Dome
43 Concordia observatory to supplement the standard PCS observatory at Vostok.
44
45

46 **1. Introduction.**

47 Dungey (1961) formulated the concept of magnetic merging processes taking place at the front of
 48 the magnetosphere between the Interplanetary Magnetic Field (IMF), when southward oriented, and
 49 the geomagnetic field, followed by the draping of the combined solar and geomagnetic fields and
 50 associated ionized plasma over the poles creating an elongated magnetospheric structure. In the
 51 extended magnetospheric tail region the geomagnetic field would reconnect releasing the solar
 52 magnetic fields. The restored geomagnetic field would then be convected sunward at lower latitudes
 53 to resume merging with the solar wind field at the front of the magnetosphere.

54 The high-latitude antisunward ionospheric and magnetospheric plasma drift across the polar cap and
 55 the return flow in the sunward motion along dawn and dusk auroral latitudes generate the two-cell
 56 “forward convection” patterns, now termed DP2 (Polar Disturbance type 2). Later, Dungey (1963)
 57 extended his model to include cases where IMF is northward (NBZ conditions), which in stronger
 58 cases would reverse the convection patterns in the central polar cap and generate sunward transpolar
 59 plasma flow (DP3) possibly inside a residual two-cell forward convection system. Although many
 60 details have been added later, these solar wind-magnetosphere interaction models still prevail now,
 61 60 years later. The strictly southward or northward IMF directions in the idealized models have
 62 been extended to all IMF directions while retaining the basic features of northward vs. southward
 63 IMF orientation.

64 The present versions of the Polar Cap (PC) index are based on the formulation by Troshichev et al.
 65 (1988) for the version developed at the Arctic and Antarctic Research Institute (AARI). The new
 66 idea was the scaling on a statistical basis of the ground magnetic variations to the merging electric
 67 field, E_M , in the solar wind (Kan and Lee, 1979) in order to make the PC indices independent of
 68 local ionospheric properties and their daily and seasonal variations. Furthermore, for the scaling of
 69 PC index values they used components of the magnetic variations in an “optimal direction”
 70 assumed being perpendicular to the average DP2 transpolar convection in order to make the new
 71 index focused on solar wind-magnetosphere interactions.

72 The standard Polar Cap (PC) indices, PCN (North) and PCS (South) are derived from polar
 73 magnetic variations recorded at Qaanaaq (Thule) in Greenland and Vostok in Antarctica,
 74 respectively. The formulation of derivation procedures has taken three directions related to the
 75 contributions by Vennerstrøm (1991), Troshichev et al. (2006), and Stauning et al. (2006). The PCN
 76 and PCS versions developed at the Danish Meteorological Institute (DMI) by Stauning et al. (2006)
 77 and Stauning (2016) are modifications of the Troshichev et al (2006) index versions. The
 78 Vennerstrøm (1991) version was abandoned in 2015. A comprehensive description of different PC
 79 index versions is available in Stauning (2013b)

80 The PCN and PCS indices have been used in various versions and combinations in studies of the
 81 relations between polar cap disturbances and further activity parameters such as solar wind electric
 82 fields and magnetospheric storm and substorm indices. Thus, single-pole PC indices, particularly
 83 PCN indices, have been used widely, but also averages of PCN and PCS indices and seasonal
 84 selections (summer or winter) of indices have been used, occasionally just named “PC index”, in
 85 scientific contributions.

86 For the relations between single-pole PC indices and solar wind conditions or global magnetic
 87 disturbances there are two conceptual problems. One is the choice between the two available
 88 hemispherical indices to be used in such relations. The other is the interpretation of negative index
 89 values which could not relate directly to the inherently positive E_M values. The combination of non-
 90 negative values of PCN and PCS indices introduced by Stauning (2007) and named PCC index have

91 helped solving both problems and underlines the need for alternative PC index data sources to
 92 ensure availability of both PCN and PCS indices.

93 The present contribution presents the potential source for PCS index values in the magnetic data
 94 from Dome Concordia (Dome-C) observatory in Antarctica (Chambodut et al., 2009; Di Mauro et
 95 al., 2014) in order to enhance the reliability and availability of PCC indices to be used for solar-
 96 terrestrial sciences as well as for space weather monitoring applications. The suggestion to use data
 97 from Dome-C for an alternative PCS index was initially forwarded in Stauning (2018b). The
 98 description of the Dome-C-based PCS indices and the definition of reference levels and scaling
 99 parameters are very similar to the corresponding definitions and descriptions of Qaanaq (THL)-
 100 based PCN indices or Vostok-based PCS indices available in Stauning (2016). An extended
 101 description of the index derivation methods beyond the present work may be found in the associated
 102 Supporting Information (SI) file where the disagreements with features of the methodologies
 103 endorsed by the International Association for Geomagnetism and Aeronomy (IAGA) are also
 104 discussed. Such discussions may also be found, among others, in Stauning (2013a, 2015, 2018a,
 105 2020 and 2021a,b).

106

107

108 **2. Basic principles for calculation of Polar Cap indices.**

109 The transpolar (noon to midnight) convection of plasma and magnetic fields driven by the
 110 interaction of the solar wind with the magnetosphere is associated with electric (equivalent Hall-
 111 type) currents in the upper atmosphere in opposite directions of the flow. These currents, in turn,
 112 induce magnetic variations at ground level (Troshichev et al., 1988, 2006; Vennerstrøm, 1991) from
 113 which the Polar Cap (PC) indices are derived.

114 The steps in the calculations of PC indices may be found elsewhere, for instance in Troshichev et al.
 115 (2006) or Stauning (2006, 2016, 2018b,c, 2020). They are summarized here for convenience and
 116 further specified in the associated SI file. In order to focus on solar wind effects, the horizontal
 117 magnetic variations, $\Delta \mathbf{F} = \mathbf{F} - \mathbf{F}_{RL}$, of the recorded horizontal magnetic field vector series, \mathbf{F} , with
 118 respect to an undisturbed reference level, \mathbf{F}_{RL} , are projected to an “optimum direction” in space to
 119 provide the projected variations, ΔF_{PROJ} . The optimum direction is assumed perpendicular to the
 120 DP2 transpolar convection-related sunward currents and characterized by its angle, φ , with the
 121 dawn-dusk meridian.

122 An important parameter for the interaction between the solar wind and the magnetosphere is the
 123 solar wind merging electric field, E_M , (also termed E_{KL} ; also named “coupling function”)
 124 formulated by Kan and Lee (1979):

$$125 \quad E_M = V_{SW} \cdot (B_Y^2 + B_Z^2)^{1/2} \cdot \sin^2(\theta/2) \quad : \quad \theta = \arctan(B_Y/B_Z) \quad (1)$$

126 where V_{SW} is the solar wind velocity, B_Y and B_Z are Geocentric Solar-Magnetosphere (GSM)
 127 components of the Interplanetary Magnetic Field (IMF), while θ is the polar angle of the transverse
 128 IMF vector. The merging electric field is supposed to control the rate of merging (coupling)
 129 between solar wind and geospace magnetic fields at the front of the magnetosphere and thereby in
 130 control of the input of solar wind energy to the Earth’s magnetosphere.

131 In consequence, the projected polar cap magnetic disturbances, ΔF_{PROJ} , are assumed being
 132 proportional to E_M :

$$133 \quad \Delta F_{PROJ} = \alpha \cdot E_M + \beta \quad (2)$$

134 where α is the slope and β the intercept parameter named from a graphical display of the relation.

135 The Polar Cap (PC) index is now defined by equivalence with E_M in the inverse relation of Eq. 2,
 136 i.e.:

$$137 \quad PC = (\Delta F_{\text{PROJ}} - \beta) / \alpha \quad (\approx E_M) \quad (3)$$

138 With the relation in Eq. 3, the ΔF_{PROJ} scalar values are scaled to make the PC index equal (on the
 139 average) to values of E_M in the solar wind. The scaling of the polar cap magnetic disturbances to a
 140 quantity in the solar wind removes (in principle) the dependence on the daily and seasonally
 141 varying ionospheric conductivities and other local conditions such as the location of the measuring
 142 polar magnetic observatory.

143

144

145 3. Handling of geomagnetic observations.

146 The magnetic data used for the standard PCN indices are collected from Qaanaaq observatory in
 147 Greenland operated by the Danish Meteorological Institute (DMI) while the Danish Space Research
 148 Institute (DTU Space) operates the magnetic instruments and takes care of the data collection and
 149 processing. Data for the standard PCS indices are collected from Vostok observatory operated by
 150 the Arctic and Antarctic Research Institute (AARI) in St. Petersburg while data for an alternative
 151 PCS index are collected from the French-Italian Dome Concordia (Dome-C) observatory.
 152 Characteristics of the three locations including essential geomagnetic parameters based on the
 153 NASA VITMO application for 2021 are specified in Table 1.

154

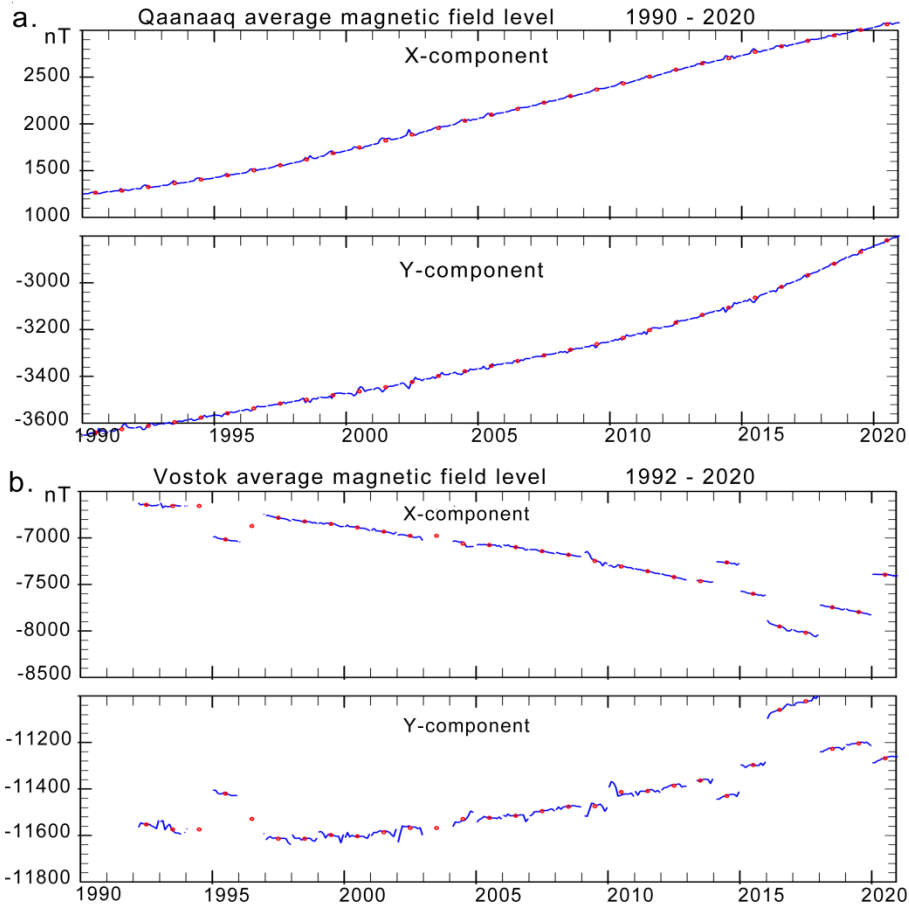
155 **Table 1.** Geographic and geomagnetic parameters at 100 km of altitude for selected stations.

Observatory	Station	Latitude	Longitude	CGMlat	CGMlon	LT=00	MLT=00
Name	Acr.	Deg.	Deg.	Deg.	Deg.	UThrs	UThrs
Qaanaaq	THL	77.47	290.77	83.86	23.86	4.62	3.60
Dome-C	DMC	-75.25	124.17	-89.31	44.52	15.72	1.77
Vostok	VOS	-78.46	106.84	-84.04	56.64	16.88	0.95

156

157 The magnetic data are carefully examined prior to their use in PC index calculations. It is of major
 158 importance that the base level values are correctly adjusted. In order to disclose possible problems,
 159 the monthly average X- and Y-component values are inspected. These values are derived as the
 160 means of measured values for all hours of the 5 quietest (QQ) days each month defined by the
 161 International Service for Geomagnetic Indices (ISGI). Figs. 1a,b display the average values for the
 162 observed X and Y components from Qaanaaq (THL) and Vostok (VOS).

163

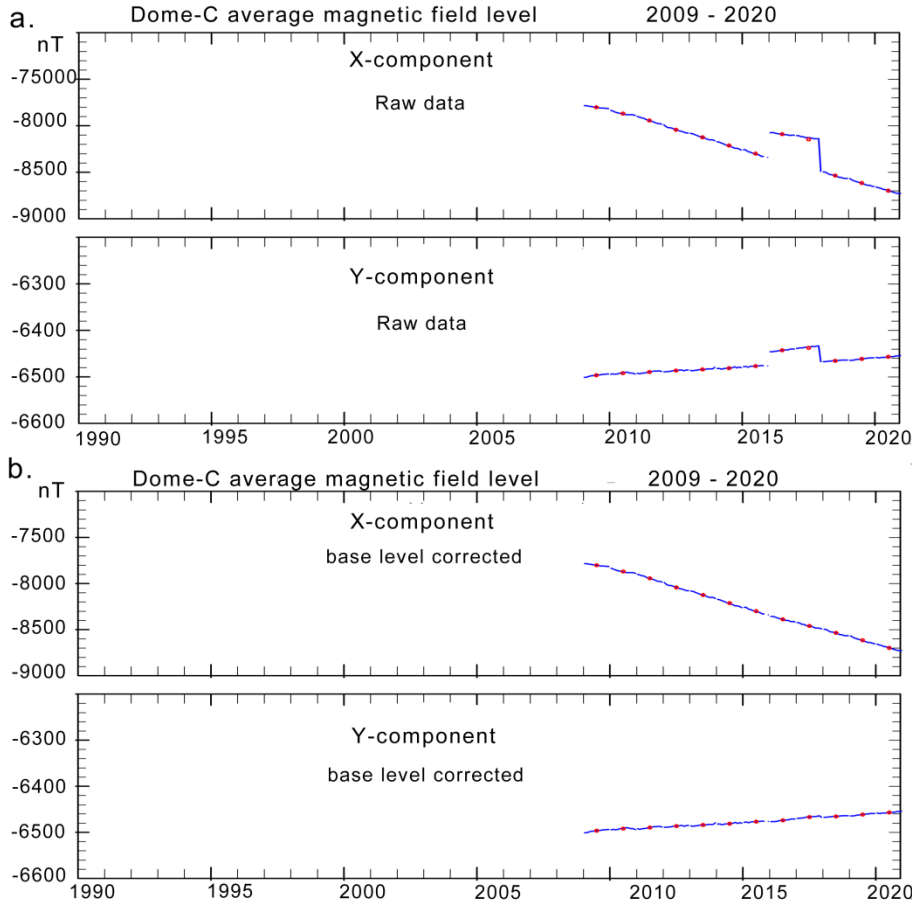


164
165

166 **Fig. 1.** Monthly (blue line) and yearly (red dots) average X- and Y-component values compiled throughout
167 all hours of the 5 quietest days each month (<http://isgi.unistra.fr>). (a) Qaanaaq (THL). (b) Vostok (VOS).
168 (data from <https://intermagnet.org>).
169

170 It is evident from Fig. 1b that the definition of proper baseline values for Vostok present challenges.
171 The base levels need comprehensive adjustments to remove irregular base level changes and retain
172 secular variations only. Such adjustments are described (to some length) in Stauning (2016). The
173 problem and possible base level corrections are not discussed at all in available reports from the
174 IAGA-endorsed PC index providers at AARI and the Danish Space Research Institute, DTU Space,
175 (e.g., Troshichev, 2011, 2017; Troshichev and Janzhura, 2012; Matzka, 2014). The base level
176 problems and occasional missing data supply from Vostok observatory underline the need for
177 alternative PCS index sources.

178 Corresponding data from Dome-C observatory are displayed in Fig. 2a. In these data there are
179 obvious base level problems during 2016-2017. However, for Dome-C data the adjustments are
180 simple and the data quality is otherwise good. The monthly and yearly average data values after
181 level correction are displayed in Fig. 2b.
182



183
184

185 **Fig. 2.** Monthly (blue line) and yearly (red dots) average X- and Y-component values compiled throughout
186 all hours of the 5 quietest days each month. (a) Dome-C measurements (data from <https://intermagnet.org>).
187 (b) Dome-C data with base level corrections.

188

189

190 4. Reference level (QDC) for PC index calculations in the SRW version.

191 The definition of reference levels, F_{RL} , to be used for calculations of the polar magnetic variations
192 needed for PC index calculations differs among the PC index versions. In the version developed at
193 AARI, the varying level on “*extremely quietest days*” (Troshichev et al., 2006) was used as the
194 data reference level. This level could be considered built from a quiet day curve (QDC), F_{QDC} ,
195 added on top of the base level, F_{BL} . Thus, in vector formulation:

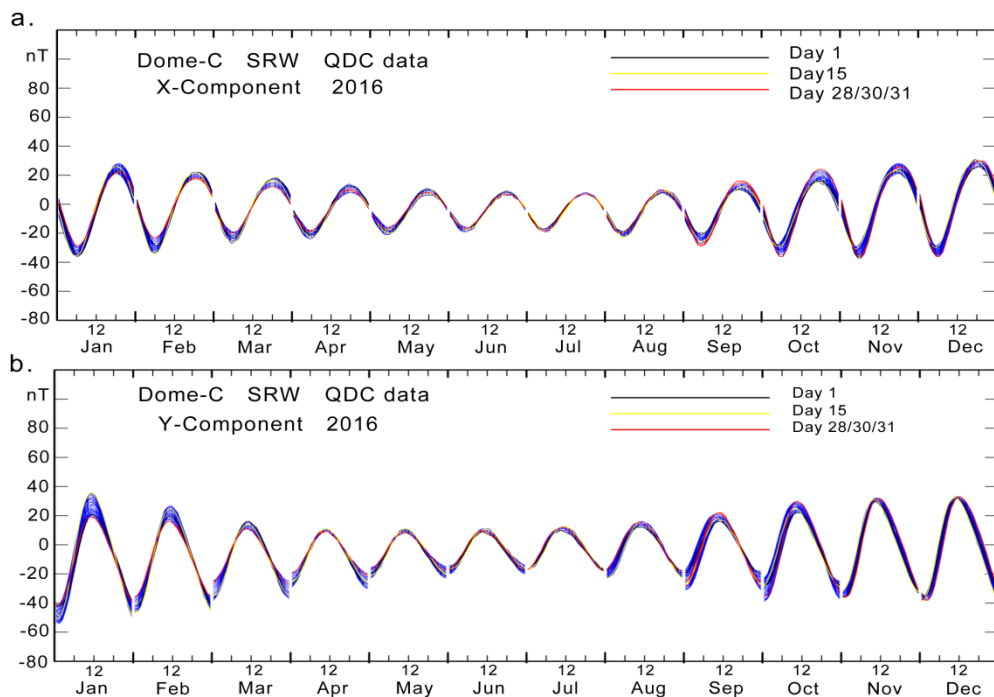
$$196 \quad F_{RL} = F_{BL} + F_{QDC} \quad (4)$$

197 Extremely quietest days are particularly rare at polar latitudes. Therefore, the concept was
198 broadened to imply the generation of QDC values from quiet segments of nearby days within 30
199 days at a time (Troshichev et al, 2006; Janzhura and Troshichev, 2008). The use of an interval close
200 to the solar rotation period (~ 27.4 days) with equal weight on each day’s quiet samples removes
201 most solar rotation effects from the QDCs.

202 The definition of the reference level is one of the issues that distinguish the PC index version
203 presented in Stauning (2016) and used in the present work from the IAGA-endorsed PC index
204 versions. The reference level construction used here (Eq. 4) is based on the formulation in

205 Troshichev et al. (2006) but uses the “solar rotation weighted” (SRW) QDC construction published
 206 in Stauning (2011) instead of the 30-days equal weight QDC methods detailed in Janzhura and
 207 Troshichev (2008) or the version with the added solar sector (SS) term detailed in Janzhura and
 208 Troshichev (2011), Matzka and Troshichev (2014), and Nielsen and Willer (2019).

209 As formulated in Stauning (2011, 2020), the essential point for the SRW method is deriving the
 210 reference level from quiet samples collected on nearby days at conditions otherwise as close as
 211 possible to those prevailing at the day of interest. Weight functions are defined to optimize the
 212 effects on the QDCs with respect to sample separation and solar rotation (see details in the SI file).
 213 For each hour of the day, observed hourly average values at corresponding hours within an
 214 extended interval (± 40 days) are multiplied by the relevant weights, added and then divided by the
 215 sum of weights to provide hourly QDC value. Subsequently, the hourly QDC values are smoothed
 216 to remove irregular fluctuations and interpolated to provide any more detailed resolution as
 217 required. The derived QDCs are routinely displayed in yearly plots for each component like the
 218 example shown in Fig. 3.
 219



220
221

222 **Fig. 3.** One year’s (2016) QDC values for Dome-C (DMC). The monthly assemblies of daily QDCs are
 223 displayed in blue lines. The QDC values on day 1, 15, and the last day of the month are superposed in black,
 224 yellow, and red lines, respectively. (a) X-component. (b) Y-component.

225

226 In these diagrams for the magnetic data from Dome-C (DMC) there is a QDC curve for each day of
 227 the year. For one month at a time, the daily QDC curves are drawn on top of each other in blue line.
 228 For day 1 (in black line), day 15 (yellow), and last day of the month (in red line) the QDCs are re-
 229 drawn on top of the other QDCs. Going from the black through the yellow to the red curves
 230 provides an impression of the development of the QDCs throughout the month. The seasonal
 231 variations are very distinct with amplitude maxima at local summer. Most of the additional
 232 variability in the QDCs is caused by the IMF B_Y -related solar sector effects which are taken into
 233 account this way.

234 The weighting over ± 40 days makes the determination of the final QDC fairly insensitive to
235 intervals of missing data. Thus, the weighting technique allows calculations of real-time QDCs with
236 reduced accuracy from past data collected within -40 to 0 days (actual time) by simply ignoring the
237 not yet available post-event samples without changing the ± 40 days' calculation scheme. As further
238 data arrive, then the QDCs could be gradually improved to be completed after passing +40 days
239 with respect to the day of interest. Thus, there are seamless transitions between real-time and post-
240 event QDC values.

241

242

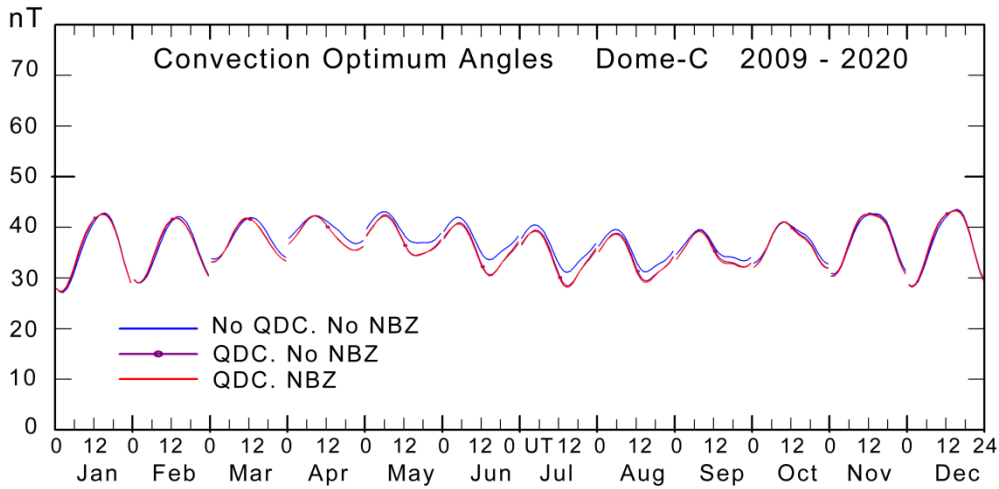
243 **5. Optimum angle calculations.**

244 At the correlation studies by Stauning (2016) using 5-min samples, the best correlations between
245 OMNI Bow Shock Nose (BSN) values of E_M and Qaanaaq ground-based ΔF_{PROJ} data series were
246 obtained for delays close to 20 min.

247 With the delay fixed, the optimum direction angles are now derived by the method defined in
248 Stauning (2016). For each calendar month and each UT hour of the day and with steps of 10° in the
249 optimum direction angle through all possible directions, the disturbance vectors, ΔF , are projected
250 to the optimum direction while the correlations between the projected magnetic disturbances and
251 the solar wind merging electric fields are calculated using textbook's product-momentum formula.

252 Among the calculated values of the correlation coefficients derived through all steps in optimum
253 direction angle, the maximum value is found. Based on the direction angle for this maximum value
254 along with the angles for the preceding and the following values of the correlation coefficient, a
255 parabolic function is then adapted to determine the precise values of the optimum direction angle at
256 the top of the parabola and the corresponding maximum correlation coefficient for the calendar
257 month and UT hour in question.

258 In order to make the values generally representative some averaging and smoothing is necessary. In
259 the present version, the values are exposed to bivariate Gaussian smoothing over months and UT
260 hours by weighted averaging. The exponents used in the smoothing weight functions characterize
261 the degree of smoothing and are stored with the derived optimum direction values. The resulting
262 mean hourly optimum angles for cases without QDC adjustments and excluding NBZ reverse
263 convection samples (blue line), with QDC and without NBZ samples (magenta line with dots), and
264 with QDC and including NBZ samples (red line) are displayed for each calendar month in Fig. 4
265



266
267

268 **Fig. 4.** Monthly mean daily variation in optimum angles for Dome-C for each month of the year. Angles
269 have been derived by using DMI2016 methods without QDC adjustments and without NBZ samples (blue
270 line), with QDC and without NBZ (magenta), with QDC and with NBZ samples (red).

271

272

273 6. Calculations of slope and intercept

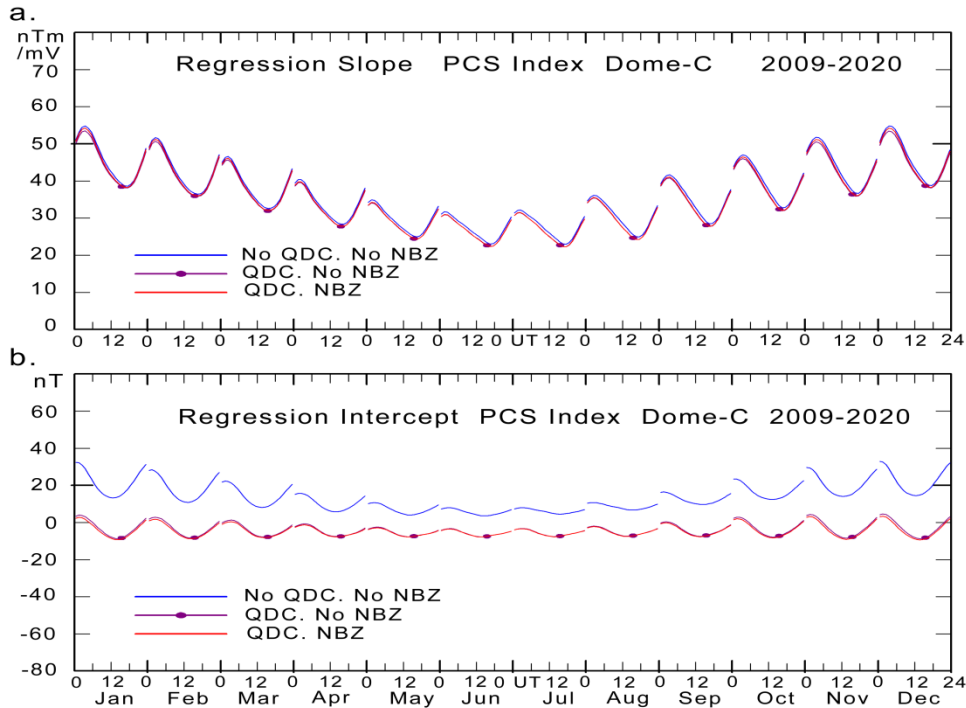
274 Recalling that we are searching for proxy values based on polar magnetic disturbances to represent
275 the solar wind "merging" electric field ($E_M = E_{KL} = V_{SW} B_T \sin^2(\theta/2)$), the general assumption is that
276 there is a (statistical) linear relation between the polar magnetic variations, ΔF_{PROJ} , and the solar
277 wind electric field, E_M , and that this relation can be inverted and used to define a polar cap (PC)
278 index by equivalence (cf. Eqs. 1-3). Contrary to the calculation of the optimum direction, the QDC
279 issue has considerable importance for the calculations of slope and intercepts parameters.

280 To solve for the coefficients in the linear relation ($\Delta F_{PROJ} = \alpha E_M + \beta$), standard least squares
281 regression is applied on a comprehensive and representative data base. For each calendar month the
282 hourly values of α and β are formed by processing all 5-min values of E_M (t-20 min) and
283 corresponding ΔF_{PROJ} (t) throughout that hour of all days of the month and all years of the selected
284 epoch.

285 In order to avoid reverse convection cases in the data base used for calculations of PC index
286 coefficients, it is required for each sample that $IMF B_Z < |IMF B_Y| + 3.0$ nT. This condition
287 excludes cases where strong northward B_Z is the dominant IMF component. A further condition
288 imposed on the selection of data requires that the projected magnetic variation, ΔF_{PROJ} , is larger
289 than the value corresponding to $PC = -2$ mV/m (≈ -50 nT). This condition ensures that cases with
290 strong reverse convection, which may continue for a while after the driving northward IMF
291 parameter has been reduced or has changed polarity, are also omitted.

292 The raw (non-smoothed) values of the slopes and intercept coefficients are exposed to bivariate
293 Gaussian smoothing over months and UT hours by weighted averaging (Stauning, 2016). The
294 resulting slope and intercept values for epoch 2009-2020 are presented in Fig. 5 in the format
295 corresponding to Fig. 4. Each of the 12 monthly sections presents the mean hourly variation in the
296 parameters for the (calendar) month. The monthly mean hourly values of the slopes and intercepts
297 are converted into series of hourly values for each (calendar) day of the year by Gaussian bivariate

298 weight function interpolation. For finer resolutions, e.g., 5-min or 1-min samples, a simple
 299 parabolic or linear interpolation is used. (Stauning, 2016).
 300



301
 302

303 **Fig. 5.** PCS slope and intercept values derived by regression of ΔF_{PROJ} on E_M with data from Dome-C
 304 (DMC) for epoch 2009-2020. Data processed without QDC involvement and without NBZ samples are
 305 displayed in blue line; data with QDC and without NBZ samples in magenta line with dots; data with QDC
 306 and including NBZ samples in red line.
 307

308 It is seen from Fig. 5 that the slope values are little affected whether the data are handled with or
 309 without QDC. The intercept values without QDC involvement (blue line) are increased by an
 310 amount representing the projected QDC contribution while including the NBZ samples (red line)
 311 has no significant effects on slope or intercept. Due to its proximity to the magnetic pole the amount
 312 and the intensities of reverse convection events are minimal at Dome-C which makes the station an
 313 ideal location for supply of data for PCS calculations. The calibration parameters are not invariant
 314 to general changes in solar activity or to secular variations in the local polar magnetic configuration,
 315 but they are kept invariant over years unless a new index version is implemented.
 316

316

317

318 7. Calculation of PC index values post event and in real time.

319 With the DMI methods (Stauning, 2016), detailed in the SI file, the scaling parameters, (φ, α, β) , are
 320 derived as monthly mean hourly values and then interpolated to provide tables at finer resolution as
 321 required. With the optimum angle values displayed in Figs. 4, the slope and intercept values
 322 displayed in Fig. 5, and the QDC values derived by the solar rotation weighted (SRW) method
 323 described in the SI file, it is now possible to calculate PCS index values vs. UT time and date. The
 324 magnetic variations are derived from the observed values by subtracting base line and QDC values.

325 The projection angle for the projection of the horizontal magnetic variation vector, $(\Delta F_X, \Delta F_Y)$, in
 326 the (rotating) observatory frame at longitude, λ , to the optimum direction, ϕ , in space is defined by:

$$327 \quad V_{\text{PROJ}} = \text{Longitude}(\lambda) + \text{UT} \cdot 15^\circ + \text{optimum direction angle}(\phi) \quad (5)$$

328 using the tabulated optimum angles (ϕ) while UT is the UT time at the observatory in hours.

329 Thus, the projected magnetic variations could be expressed by:

$$330 \quad \Delta F_{\text{PROJ}} = \Delta F_X \cdot \sin(V_{\text{PROJ}}) \pm \Delta F_Y \cdot \cos(V_{\text{PROJ}}) : (+ \text{ for southern, } - \text{ for northern hemisphere}) \quad (6)$$

331 The slope and intercept values, α and β are fetched from their tabulated values to be used in Eq. 3
 332 defining PC index values ($\text{PC} = (\Delta F_{\text{PROJ}} - \beta) / \alpha$)

333 For real-time applications the critical issue is defining the undisturbed reference level. For the
 334 present approach the QDC values are derived by the (half interval) HSRW method using quiet
 335 samples collected from past data only during the interval from -40 to 0 days (see SI file). A detailed
 336 description of methods for current calculations of QDC values and PC indices in real-time may be
 337 found in the appendix to Stauning (2018c).

338

339

340 **8. Assessments of PC index quality.**

341 For a geophysical index offered to the international scientific community and important space
 342 weather services, the quality of the post event (definitive) as well as the real-time (prompt) index
 343 values is of utmost importance. In spite of this (seemingly) obvious ascertainment, little efforts have
 344 been provided on this issue at past and present PC index versions.

345 The main quality principles were formulated in Troshichev et al. (1988).

346 “- PC index in any UT time should be determined by the polar cap magnetic disturbance value
 347 related to influence of the geoeffective solar wind, and therefore

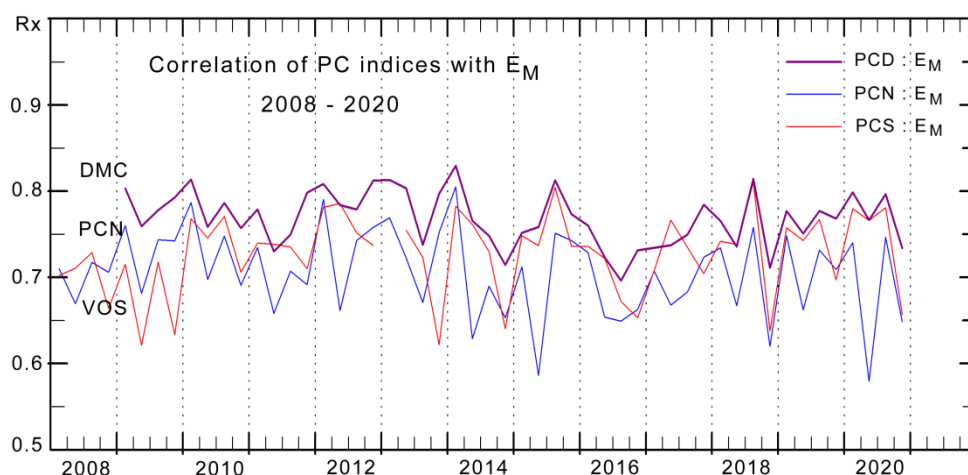
348 - the magnetic disturbance vector δF should be counted from level of the quiet geomagnetic field to
 349 eliminate variations unrelated to the solar wind fluctuations;

350 - PC index should correspond to the value of the interplanetary electric field E_{KL} (E_M) impacting the
 351 magnetosphere, irrespective of UT time, season and point of observation.”

352 The reference levels advocated here are by their definition (cf. section 5) based on quiet (the
 353 quietest) geomagnetic samples and thus they comply with the quality requirements.

354 The correlations between 15-min average values of Dome-C-based PCS index values (PCD) and
 355 values of the merging electric field shifted by 20 min are displayed in Fig. 6. The quarterly mean
 356 correlation coefficients between 15-min E_M values and PCS values based on Dome-C data are
 357 displayed in heavy magenta line while the corresponding correlation coefficients for Vostok-based
 358 PCS values are displayed in red line and the coefficients for Qaanaaq (THL)-based PCN values are
 359 shown in blue line.

360

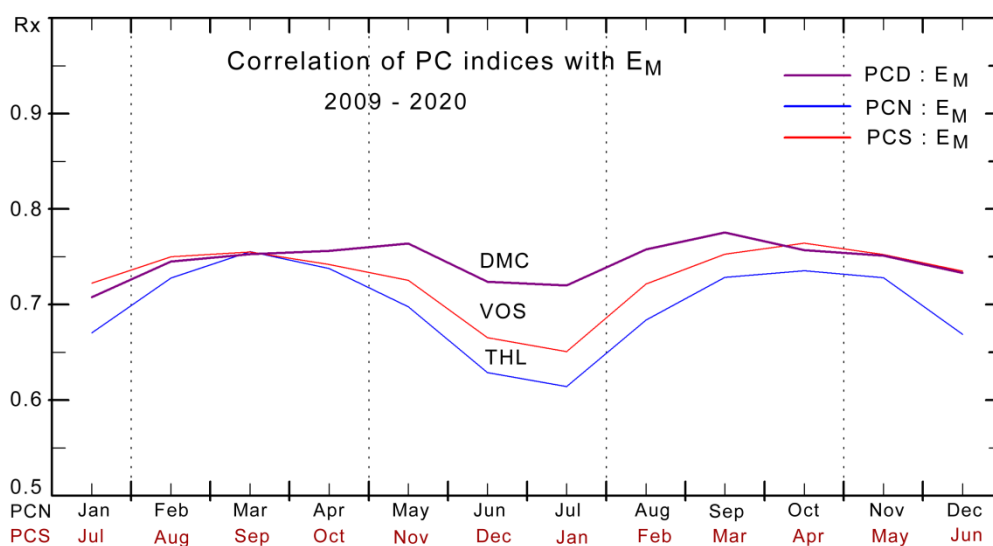


361
362

363 **Fig. 6.** Quarterly means of coefficients for the correlation between 15-min averages of the merging
364 electric field, E_M , and Dome-C-based PCS values (PCD) in heavy magenta line and corresponding
365 coefficients for Vostok-based PCS values (red line) and Qaanaaq-based PCN values (blue line).
366

367 With a single exception in 2017, the correlation between 15-min E_M and Dome-C based PCS values
368 seen in Fig. 6 is higher – at times much higher – than the correlation between E_M and the Vostok-
369 based PCS values and consistently much higher than the correlation between E_M and the Qaanaaq
370 (THL)-based PCN values throughout the epoch (2009-2020).

371 The seasonal variations in the correlation between E_M and the PC indices are displayed in Fig. 7 by
372 the monthly mean correlation coefficients for 15-min samples averaged over the epoch 2009-2020.
373 The line types are the same as those used in Fig. 6. The order of southern months has been
374 rearranged to make seasons match.
375



376
377

378 **Fig. 7.** Monthly means of coefficients for the correlation between 15-min averages of E_M and Dome-C-based
379 PCS values (PCD) in heavy magenta line. Corresponding coefficients for Vostok-based PCS values in red
380 line and Qaanaaq-based PCN values in blue line. The order of southern months has been rearranged.
381

382 It is seen from Fig. 7 that the coefficients for the correlation between E_M and PCS values based on
 383 Dome-C data are close to the corresponding values for PCS indices based on Vostok data
 384 throughout the local winter months (April-September) but much higher at local summer (October-
 385 March). The correlation coefficients between E_M and Qaanaaq-based PCN index values are much
 386 lower than either E_M - PCS correlations during most of the year.

387 The main reason for the low correlations during local summer months is the increased occurrence
 388 frequencies and enhanced intensities of reverse convection events compared to conditions at (local)
 389 winter. In terms of location, such reverse convection events are particularly frequent and intense
 390 midway between the Cusp region at the dayside and the geomagnetic pole. Thus, they are less
 391 frequent and intense at Vostok compared to Qaanaaq and furthermore less frequent at Dome-C
 392 compared to Vostok due to the closer proximity to the (southern) geomagnetic pole (cf. Table 1).

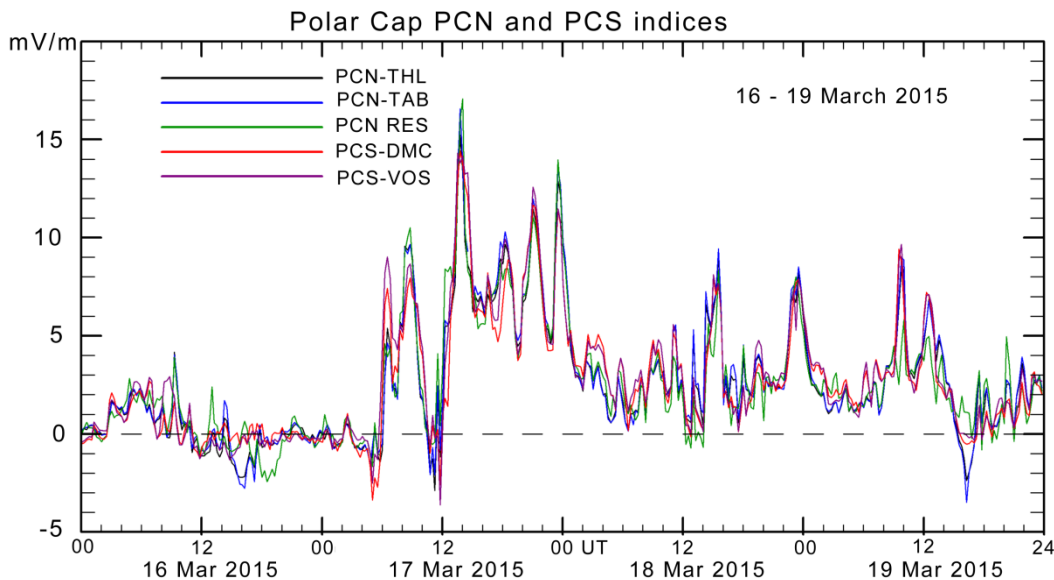
393

394

395 9. Examples of Dome-C-based PCS indices.

396 The availability of magnetic observations and the derivation of calibration parameters from Dome
 397 Concordia data are important for reliable investigations of space weather effects by providing back-
 398 up for the PCS index values particularly in cases where the harsh arctic environment may inhibit
 399 supply of data from Vostok or invalidate data quality. Correspondingly, the supply of data for PCN
 400 index values might be consolidated by using alternative sources of magnetic data such as Resolute
 401 Bay (RES) in Canada or Thule Air Base (TAB) in Greenland (Stauning, 2018b). An example of
 402 PCN and PCS values compiled from these sources is displayed in Fig.8 for the strong magnetic
 403 storm ($Dst(\min) = -222$ nT) on 16-19 March 2015.

404



405

406

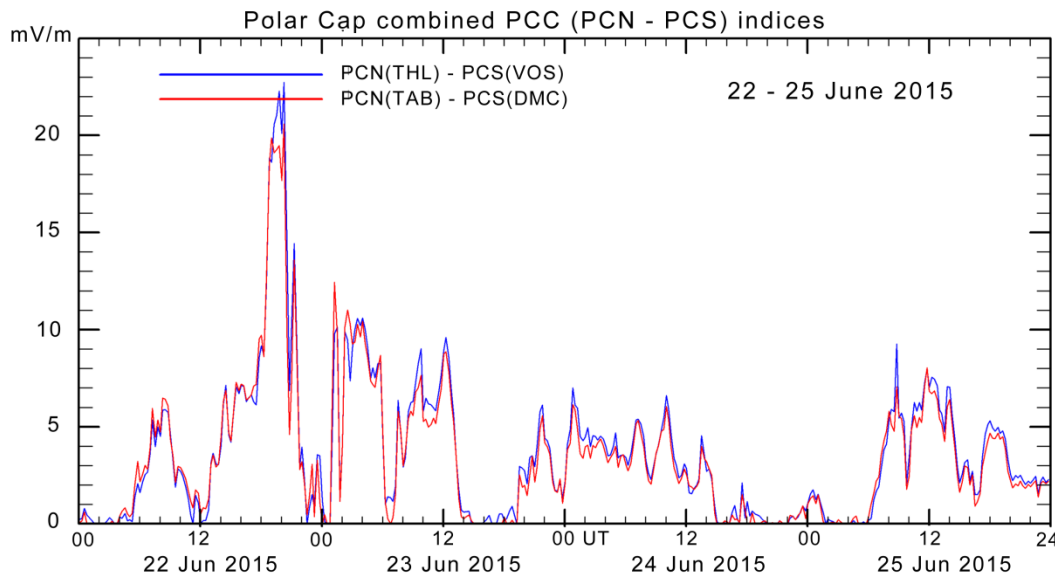
407 **Fig. 8.** Example of PCN and PCS values calculated in the “DMI2016” index versions for 4 days, 16-19
 408 March 2015, of a strong magnetic storm event ($Dst(\min) = -222$ nT).

409

410 It is evident from Fig. 8 that the main polar convection parameters such as the PCC indices
 411 (Stauning, 2007, 2012, 2021c, 2021d; Stauning et al., 2008) which need available PCN as well as

412 PCS indices could be restored with high confidence from the abundance of index sources even in
 413 the absence of a single data source.

414 In the strong and complex magnetic storm on 23-26 July 2015 ($Dst(\min) = -204$ nT), the Qaanaaq-
 415 based PCN indices have been combined with the Vostok-based PCS indices to form the PCC
 416 indices displayed in blue line while the Thule AB-based PCN indices have been combined with the
 417 Dome-C-based PCS indices to form alternative PCC indices shown in red line. The PCN and PCS
 418 indices could be combined differently to form the dual-pole PCC indices.
 419



420
 421
 422 **Fig. 9.** Polar Cap combined (PCC) indices formed from PCN(Qaanaaq) and PCS(Vostok) indices in
 423 blue line. Alternative PCC indices formed from PCN(Thule AB) and PCS(Dome-C) in red line.
 424

425 The differences between the two alternative PCC indices are just a small fraction of their
 426 amplitudes such that either version would suffice for most space weather applications such as
 427 estimates of the solar wind energy input or ring current enhancements (Stauning, 2012, 2021a,c).

428 Furthermore, for space weather monitoring as well as for scientific investigations of solar wind-
 429 magnetosphere interactions, the double variety of index versions would provide an insurance
 430 against faulty interpretation of the situation relying on invalid data from any single source.

431

432

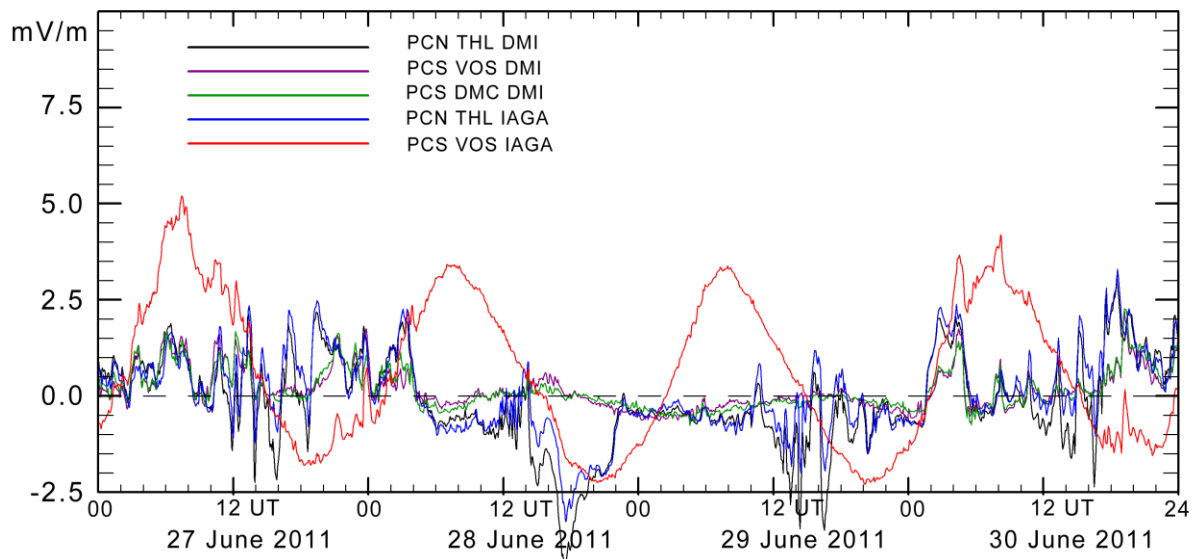
433 10. Invalid IAGA-supported PCS indices

434 In spite of IAGA support through forming the “Index Endorsement Criteria” (2009) and the PC
 435 index endorsement by Resolution #3 (2013) and furthermore the involvement in the International
 436 Service for Geomagnetic Indices (ISGI), the “official” PC index series are poorly documented and
 437 not reliable.

438 One issue is the reference level construction (Janzhura and Troshichev, 2011; Troshichev and
 439 Janzhura, 2012) that may cause unfounded changes in the reference level during several days
 440 around any particularly strong disturbance event or cause considerable changes in the night-time
 441 reference level from daytime cusp-related disturbances (see Stauning, 2013a, 2015, and 2020).
 442 Another issue is the statistical handling where the non-linear processing (smoothing) of fluctuating
 443 scaling parameters based on small initial batches of data samples generate systematic errors as
 444 documented in Stauning (2021b). A further issue is the mixing of DP2 (forward convection) and

445 DP3 (reverse convection) samples in the calculations of scaling parameters (see Stauning, 2015). A
 446 particularly alarming issue is the lack of verification of methods and control of the PC index series
 447 offered to the scientific community.

448 A striking example of invalid PCS index values is displayed in Fig. 10 with indices for 27-30 June
 449 2011 for Qaanaaq (THL), Vostok (VOS) and Dome-C (DMC) in the versions (DMI) defined in the
 450 present work and PCN and PCS index values in the IAGA-supported versions.
 451



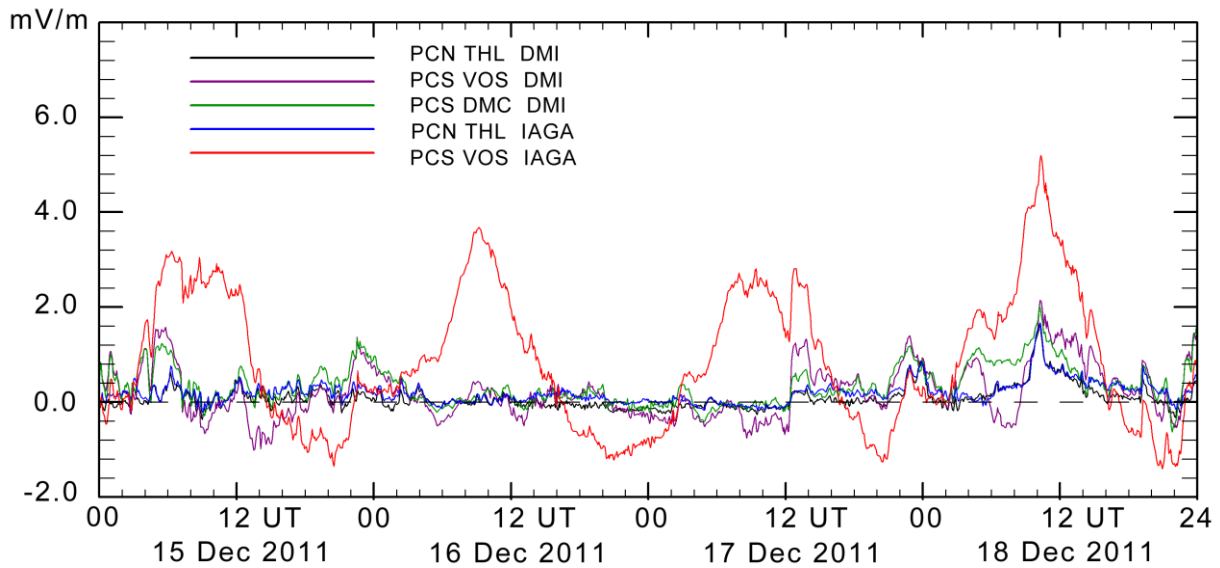
452
 453

454 **Fig. 10.** PCN and PCS index values for 27-30 June 2011 in DMI2016 versions based on data from Qaanaaq
 455 (THL) in black line, from Vostok (magenta), and from Dome-C (green). PCN and PCS index values in
 456 IAGA-supported versions based on data from Qaanaaq (blue line) and Vostok (red line).
 457

458 It is seen that the daily excursions between -2 and +4 mV/m (magnetic storm level) in the IAGA
 459 PCS values (red line) must be in error when compared to the other index values recorded on these
 460 rather quiet days. In passing it might be noted that the Vostok-based PCS indices (magenta line)
 461 agree well with the Dome-C-based PCS index values (green) in the DMI versions.

462 The PCN and PCS index values in the IAGA-supported versions (blue and red lines) were
 463 downloaded in September 2021 from the “final” version link at the AARI web site
 464 <https://pcindex.org> and confirmed by the identical index data downloaded also in September 2021
 465 from the IAGA-supported ISGI web service at (<http://isgi.unistra.fr>).

466 Corresponding features are seen in Fig. 11 holding PC index data for 15-18 December 2011. It is
 467 obvious that the daily excursions between -1 and +3 mV/m in the IAGA PCS values (red line) must
 468 be in error when compared to the other index values recorded on these very quiet days.
 469



470
471

472 **Fig. 11.** PCN and PCS index values for 15-18 December 2011 in DMI2016 versions (DMI) based on data
473 from Qaanaaq (THL) in black line, from Vostok (magenta), and from Dome-C (green). PCN and PCS index
474 values in IAGA-supported versions based on data from Qaanaaq (blue line) and Vostok (red line).
475

476 The diagram in Fig. 11 was initially presented in Stauning (2020 and 2021c) but has now been
477 redrawn with PCN and PCS index values in the IAGA-supported versions downloaded in
478 September 2021 from the “final” versions link at the AARI web site <https://pcindex.org> and (again)
479 confirmed by the identical index data from the IAGA-supported ISGI web service at
480 (<http://isgi.unistra.fr>).

481 The Vostok data from this interval (from <https://intermagnet.org>) are good (cf. Fig. 1). Thus, the
482 excessive values in the IAGA PCS data must rely on failures in the processing software which have
483 been in use since the IAGA endorsement by Resolution #3 in 2013.

484 Similar excessive PCS index values published by AARI and ISGI web services were displayed in
485 Fig. 8 of Stauning (2018b) and the failures reported to the index providers and to IAGA. There were
486 no responses from the index providers. In the reply from 21 May 2018 from IAGA EC the concerns
487 over the invalid PCS index values were dismissed. However, these erroneous PCS index data have
488 been used in a number of publications since 2013 up to now (2021), among others, in those issued
489 from AARI, which now add to the 40 devaluated publications listed in Stauning (2021b) that have
490 used PC indices in versions now known being invalid.

491
492

493 **Conclusions**

494 Due to its close proximity to the (southern) geomagnetic pole, the occurrence frequency and the
495 intensity of disturbing reverse convection events (NBZ conditions) as well as the amount of
496 interfering substorm activity are at very low levels at the Antarctic research station Dome
497 Concordia (Dome-C) making the location ideal for supply of basic magnetic data for PC indices.

498 - The characteristics of the PCS indices derived from data from Dome-C have shown that these data
499 have an unprecedented close relation to the merging electric field, E_M , in the impinging solar wind.

- 500 - It is strongly recommended that available Dome-C data (since 2009) are processed to form
 501 alternative PCS index values made available to provide substitutes for missing or poor PCS values
 502 based on data from the standard observatory, Vostok.
- 503 - Alternative Dome-C-based PCS index values may form reassuring validation when agreeing with
 504 the standard PCS indices based on Vostok magnetic data or provide motivation for critical
 505 examination of data and processing procedures in cases of disagreements.
- 506 - It is suggested that efforts are invested in making data from Dome-C available in real-time and
 507 that processing procedures like those presented here are established to generate real-time Polar Cap
 508 (PCS) indices for space weather monitoring.
- 509 - The present work (including its SI file) provides coherent definitions and detailed descriptions of
 510 all steps involved in the generation of Polar Cap (PC) index scaling parameters and index values in
 511 their post-event and real-time versions.
- 512 - It is disappointing that IAGA upon endorsing the current “official” PC index versions by its
 513 Resolution #3 (2013) has failed to request comprehensive documentation of derivation procedures,
 514 proper validation of methods, and effective quality control of published index series supplied to the
 515 international scientific community.

516

517

518 **Data availability:**

519 Near real-time (prompt) PC index values and archived PCN and PCS index series derived by the
 520 IAGA-endorsed procedures are available through AARI and ISGI web sites. Archived PCN and
 521 PCS data used in the paper were downloaded from the “final” version link at <https://pcindex.org> and
 522 from <http://isgi.unistra.fr> in September 2021 unless otherwise noted.

523 Space data from the WIND, ACE, and GeoTail missions for deriving E_M and IMF B_Y values have
 524 been obtained from OMNIweb space data service at <https://omniweb.gsfc.nasa.gov> .

525 Geomagnetic data from Qaanaaq, Vostok and Dome-C were provided from the INTERMAGNET
 526 data service web portal at <https://intermagnet.org> .

527 The observatory in Qaanaaq is managed by the Danish Meteorological Institute, while the
 528 magnetometer there is operated by DTU Space, Denmark. The Vostok observatory is operated by
 529 the Arctic and Antarctic Research Institute in St. Petersburg, Russia. The Dome-C observatory is
 530 managed by Ecole et Observatoire des Sciences de la Terre (<https://eost.unistra.fr>) (France) and
 531 Istituto Nazionale di Geofisica e Vulcanologia (<https://ingv.it>) (Italy).

532 The “DMI2016” PC index version is documented in the report DMI SR-16-22 (Stauning, 2016)
 533 available at the web site: https://www.dmi.dk/fileadmin/user_upload/Rapporter/TR/2016/SR-16-22-PCindex.pdf

534
 535 Details of the Dome-C-based PCS index definitions and derivation methods are provided in the
 536 accompanying Supporting Information file.

537

538

539 **Conflict of interest**

540 The author declares that he has no conflict of interests related to the present submission.

541

542

543 **Acknowledgments.** The staffs at the observatories in Qaanaaq (Thule), Vostok, and Concordia and
 544 their supporting institutes are gratefully acknowledged for providing high-quality geomagnetic data
 545 for this study. The space data contributions managed through OMNIweb data center from the ACE,
 546 GeoTail, and WIND spacecraft missions are gratefully acknowledged. The efficient provision of
 547 geomagnetic data from the INTERMAGNET data service centre, and the excellent performance of
 548 the PC index portals are greatly appreciated. The author gratefully acknowledges the collaboration
 549 and many rewarding discussions in the past with Drs. O. A. Troshichev and A. S. Janzhura at the
 550 Arctic and Antarctic Research Institute in St. Petersburg, Russia.

551

552

553 **References**

- 554 Chambodut A, Di Mauro D, Schott JJ, Bordais P, Agnoletto L, Di Felice P. (2009). Three years
 555 continuous record of the Earth's magnetic field at Concordia station (Dome-C, Antarctica).
 556 *Annals of Geophysics* **52** 15-24. <https://doi.org/10.4401/ag-4569> .
- 557 Di Mauro D, Cafarella L, Lepidi S, Pietrolungo M, Alfonsi L, Chambodut A. (2014). Geomagnetic
 558 polar observatories: the role of Concordia station at Dome C, Antarctica, *Annals of Geophysics*
 559 **57**, 6, G0656. <https://doi.org/10.4401/ag-6605> .
- 560 Dungey J. W. (1961). Interplanetary Magnetic Field and the Auroral Zones. *Phys Rev Lett* **6**, 47-48.
 561 <https://doi.org/10.1103/PhysRevLett.6.47> .
- 562 Dungey, J. W. (1963). The structure of the ionosphere or adventures in velocity space, in:
 563 *Geophysics: The Earth's environment*. Ed. by Dewitt, C., Hiebolt, J. & Lebeau, A., pp. 526-536,
 564 Gordon and Breach, New York.
- 565 IAGA Resolution no. 3 (2013). <http://www.iaga-aiga.org/resolutions>.
- 566 IAGA Index endorsement criteria (2009).
 567 https://www.ngdc.noaa.gov/IAGA/vdat/GeomagneticIndices/Criteria_for_Endorsement.pdf
- 568 Janzhura, A.S. & Troshichev, O.A. (2008). Determination of the running quiet daily geomagnetic
 569 variation, *J Atmos Solar-Terr Phys* **70**, 962–972, <https://doi.org/10.1016/j.jastp.2007.11.004>
- 570 Janzhura, A.S. & Troshichev, O.A. (2011). Identification of the IMF sector structure in near-real
 571 time by ground magnetic data. *Annales Geophysicae* **29** 1491-1500.
 572 <https://doi.org/10.5194/angeo-29-1491-2011> .
- 573 Kan, J. R. & Lee, L. C. (1979). Energy coupling function and solar wind-magnetosphere dynamo.
 574 *Geophysical Research Letter*, **6** (7), 577- 580. <https://doi.org/10.1029/GL006i007p00577> .
- 575 Matzka, J. (2014). PC index description and software. <https://doi.org/10.11581/DTU:00000057>
- 576 Matzka, J. & Troshichev, O.A. (2014). PC index description main document and references.
 577 http://isgi.unistra.fr/Documents/References/PC_index_description_main_document.pdf
- 578 Nielsen, J. B. & Willer, A. N. (2019). Restructuring and harmonizing the code used to calculate the
 579 Definitive Polar Cap Index. *Report from DTU Space*. <https://tinyurl.com/sx3g5t5>
- 580 Stauning, P. (2007). A new index for the interplanetary merging electric field and the global
 581 geomagnetic activity: Application of the unified Polar Cap (PCN and PCS) indices. *AGU Space*
 582 *Weather*, **5**, S09001. <https://doi.org/10.1029/2007SW000311> .
- 583 Stauning, P. (2011). Determination of the quiet daily geomagnetic variations for polar regions. *J.*
 584 *Atmos Solar-Terr Phys*, **73**(16), 2314-2330. <https://doi.org/10.1016/j.jastp.2011.07.004> .

- 585 Stauning, P. (2012). The Polar Cap PC Indices: Relations to Solar Wind and Global Disturbances,
 586 Exploring the Solar Wind, Marian Lazar (Ed.). *InTech Publ.* ISBN: 978-953-51-0339-4.
 587 <https://doi.org/10.5772/37359>
- 588 Stauning, P. (2013a). Comments on quiet daily variation derivation in “Identification of the IMF
 589 sector structure in near-real time by ground magnetic data” by Janzhura and Troshichev (2011).
 590 *Annales Geophysicae*, 31, 1221-1225. <https://doi.org/10.5194/angeo-31-1221-2013> .
- 591 Stauning, P. (2013b). The Polar Cap index: A critical review of methods and a new approach, *J.*
 592 *Geophys. Res. Space Physics*, 118, 5021-5038. <https://doi.org/10.1002/jgra.50462>
- 593 Stauning, P. (2015). A critical note on the IAGA-endorsed Polar Cap index procedure: effects of
 594 solar wind sector structure and reverse polar convection. *Annales Geophysicae*, 33, 1443-1455.
 595 <https://doi.org/10.5194/angeo-33-1443-2015> .
- 596 Stauning, P. (2016). The Polar Cap (PC) Index.: Derivation Procedures and Quality Control. *DMI*
 597 *Scientific Report SR-16-22*. Available at:
 598 https://www.dmi.dk/fileadmin/user_upload/Rapporter/TR/2016/SR-16-22-PCindex.pdf .
- 599 Stauning, P. (2018a). A critical note on the IAGA-endorsed Polar Cap (PC) indices: excessive
 600 excursions in the real-time index values. *Ann Geophys* 36, 621–631.
 601 <https://doi.org/10.5194/angeo-36-621-2018> .
- 602 Stauning, P. (2018b). Multi-station basis for Polar Cap (PC) indices: ensuring credibility and
 603 operational reliability. *J Space Weather Space Clim* 8, A07.
 604 <https://doi.org/10.1051/swsc/2017036> .
- 605 Stauning, P. (2018c). Reliable Polar Cap (PC) indices for space weather monitoring and forecast, *J*
 606 *Space Weather Space Clim* 8, A49. <https://doi.org/10.1051/swsc/2018031>
- 607 Stauning, P. (2020). The Polar Cap (PC) index: invalid index series and a different approach. *Space*
 608 *Weather* 16, e2020SW002442. <https://doi.org/10.1029/2020SW002442>
- 609 Stauning, P. (2021a). Comment on “Identification of the IMF sector structure in near-real time by
 610 ground magnetic data” by Janzhura & Troshichev (2011). *Ann. Geophys.*, 39, 369–377.
 611 <https://doi.org/10.5194/angeo-39-369-2021>
- 612 Stauning, P., 2021b. Invalid Polar Cap (PC) indices: Erroneous scaling parameters, *J. Geophys. Res.*
 613 *Space Phys.* <https://doi.org/10.1029/2020SW002442> .
- 614 Stauning, P. (2021c). The Polar Cap (PC) index combination, PCC: relations to solar wind
 615 properties and global magnetic disturbances. *J Space Weather Space Clim*
 616 <https://doi.org/10.1051/swsc/2020074>
- 617 Stauning, P., 2021d. Transpolar convection and magnetospheric ring currents: real-time applications
 618 of Polar Cap (PC) indices. *Space Weather.* <https://doi.org/10.1029/2020SW002072>
- 619 Stauning, P., Troshichev, O. A., & Janzhura, A. S. (2006). Polar Cap (PC) index. Unified PC-N
 620 (North) index procedures and quality. *DMI Scientific Report, SR-06-04*. (revised 2007 version
 621 available at <http://www.dmi.dk/fileadmin/Rapporter/SR/sr06-04.pdf>).
- 622 Stauning, P., Troshichev, O. A., & Janzhura, A. S. (2008). The Polar Cap (PC) index: Relations to
 623 solar wind parameters and global activity level, *J Atmos Solar-Terr Phys* 70(18), 2246-2261.
 624 <https://doi.org/10.1016/j.jastp.2008.09.028> .
- 625 Troshichev, O. A. (2011). Polar Cap (PC) Index. Available at: <https://pcindex.org> (see Supported
 626 materials).
- 627 Troshichev, OA (2017). Polar cap magnetic activity (PC index) and space weather monitoring,
 628 *Édition universitaires européennes*, ISBN: 978-3-8381-8012-0.

- 629 Troshichev, O. A. & Janzhura, A. S. (2012). Space Weather monitoring by ground-based means,
630 *Springer Praxis Books*, Heidelberg, ISBN 978-3-642-16802-4, [https://doi.org/10.1007/978-3-](https://doi.org/10.1007/978-3-642-16803-1)
631 [642-16803-1](https://doi.org/10.1007/978-3-642-16803-1), 2012.
- 632 Troshichev, O. A., Andrezen, V. G., Vennerstrøm, S. & Friis-Christensen, E. (1988). Magnetic
633 activity in the polar cap – A new index. *Journal of Planetary and Space Sciences* 36(11), 1095-
634 1102. [https://doi.org/10.1016/0032-0633\(88\)90063-3](https://doi.org/10.1016/0032-0633(88)90063-3)
- 635 Troshichev, O. A., Janzhura, A. S., Stauning, P. (2006). Unified PCN and PCS indices: method of
636 calculation, physical sense and dependence on the IMF azimuthal and northward components, *J.*
637 *Geophys. Res.*, 111, A05208, <https://doi.org/10.1029/2005JA011402>, 2006. (correction in
638 Troshichev et al., 2009)
- 639 Troshichev, O. A., Janzhura, A. S., Stauning, P. (2009). Correction to “Unified PCN and PCS
640 indices: Method of calculation, physical sense, and dependence on the IMF azimuthal and
641 northward components, *J. Geophys. Res.*, 111, A05208”, *J. Geophys. Res.* 114, A11202,
642 <https://doi.org/10.1029/2009JA014937>, 2009.
- 643 Vennerstrøm, S. (1991). The geomagnetic activity index PC, PhD Thesis, Scientific Report 91-3,
644 Danish Meteorological Institute, 105 pp.
645 https://www.dmi.dk/fileadmin/user_upload/Rapporter/SR/1991/sr91-3.pdf
646